Received: 22 January 2024 | *Revised:* 7 April 2024 | *Accepted:* 13 April 2024
DOI: 10.37917/ijeee.22.1.11 *Vol. 22 | Issue 1 | June 2026*

Iraqi Journal for Electrical and Electronic Engineering
Original Article

Open Access
IJEEE University of Basrah College of Engineering

Validation Analysis of Improved Skipping Algorithm for Photovoltaic Maximum Power Point Tracking System Under Partial Shading Conditions

Hameed Ali Mohammed[1,2], **Rosmiwati Mohd-Mokhtar***[1], **Hazem Ibrahim Ali**[3]
[1]School of Electrical and Electronic Engineering, Engineering Campus, Universiti Sains Malaysia, Pulau Pinang, Malaysia
[2]Petroleum Systems Control Engineering Department, University of Tikrit, Slah Al Deen, Iraq
[3]Control and Systems Engineering Department, University of Technology, Baghdad, Iraq

Correspondance
*Rosmiwati Mohd-Mokhtar
School of Electrical and Electronic Engineering, Engineering Campus,
Universiti Sains Malaysia, Pulau Pinang, Malaysia
Email: eerosmiwati@usm.my

Abstract
The efficient and fast-tracking of the global maximum power point (GMPP) under partial shading conditions (PSCs) is one of the most significant goals of the maximum power point tracking (MPPT) algorithms. This paper introduces an algorithm to identify the accurate range locations of the GMPP. A skipping MPPT algorithm is proposed to minimize the time consumed in tracking the GMPP. The proposed algorithm uses a skipping voltage method to minimize scanning the voltage range on the Power-Voltage (P-V) curve by neglecting the zones without GMPP. During GMPP tracking under PSCs, the automatic initial voltage generator algorithm ensures no overlap between two adjacent zones on the P-V curve. The proposed skipping algorithm guarantees that the GMPP is tracked accurately under all potential atmospheric circumstances with a shorter tracking time and the ability to find the GMPP quickly, minimizing the power loss. The improved performance of the proposed algorithm has been validated by simulation and experimental results on a PV string. From the results, the proposed MPPT algorithm has demonstrated its superiority in tracking the GMPP under PSCs in terms of accuracy and tracking speed compared to other MPPT algorithms. The proposed algorithm tracks the GMPP faster, with a time difference of $\Delta t = 3.28$ sec and $\Delta t = 27$ msec from the experimental and simulation results under PSCs. The proposed algorithm also successfully tracks the GMPP in the final zone, while the $0.8V_{OCM}$ MPPT algorithm fails, which causes a high-power loss of 196 watts compared to the proposed skipping algorithm.

Keywords
Global Maximum Power Point, Partial Shading Conditions, Photovoltaic, Skipping Method.

I. Introduction

Photovoltaic (PV) energy is considered one of the most attractive energy resources with many merits, such as being sustainable, environmentally friendly, producing no noise and requiring minimum maintenance. However, PV array systems have several drawbacks, such as low power conversion efficiency, so enhancing power performance under different weather conditions is necessary. The nonlinear attitude of the P-V curve for the PV array system generates only one maximum operating point, known as the maximum power point (MPP) [1–4]. The MPPT is the most significant technique for harvesting maximum power from the PV array system. Based on different climate conditions, such as ambient temperature and solar irradiation, the MPPT techniques force the PV array to work at an efficient operating point called the maximum power voltage, V_{MPP}, on the P-V curve [5–7]. Therefore, a good MPPT algorithm design is necessary to reach the MPP and maximize the power extracted

from the PV array [2, 8, 9]. The deep analysis of operating point behavior helps researchers to design a suitable MPPT algorithm, which leads the operating point to work near the MPP [10]. The conventional MPPT algorithms are the most popular for tracking the MPP due to their uncomplicated implementation and inexpensive [11, 12].

Despite these merits, the conventional MPPT algorithms suffer from two main demerits: the continuous fluctuations around the MPP even after reaching the MPP at the steady state response and the inefficiency of tracking the MPP under sudden changes in climate conditions [13, 14]. The PV modules must be connected in series and parallel to enhance the PV output power. If a series of modules receive unequal irradiation, the negative voltage would appear across the modules, which receive a lower insolation level. Also, the lower irradiation on a PV array fraction pushes the unshaded modules to operate in reverse bias, which leads to high power losses and a rise in temperature within these modules [15–17].

During PSCs, the PV array has multiple peaks on the P-V curve, several local maximum power points (LMPPs) and only one global maximum power point (GMPP) [18, 19]. The conventional MPPT algorithm is unable to identify the GMPP during PSCs. Research has been done by modifying the conventional MPPT algorithms to eliminate the weak points and make them work efficiently under multiple-peak issues [20]. Authors in [21] presented a 2-phase tracking method to enhance the tracking performance of the conventional Incremental Conductance (INC) MPPT. Even though the performance of the INC algorithm has been improved in terms of tracking speed, it is still unable to identify and track the GMPP during PSCs. In [22, 23], authors used the open circuit voltage, V_{OC} method by assuming that the GMPPs are located at $0.85V_{OC}$ or $0.8V_{OC}$ of the PV module on the P-V curve, respectively. Then, the conventional Perturb-and-Observe (P&O) MPPT algorithm tracks the GMPP inside this zone.

Based on this concept, the modified methods only search around these specific points on the P-V curve, while other voltage zones are neglected. The method is accurate only when the peaks on the P-V curve are in ascending order toward the GMPP. To guarantee tracking the GMPP, the MPPT algorithms must search the full voltage range on the P-V curve, but this procedure is time-consuming. A skipping method can reduce the searching time wasted until it reaches the GMPP. Skip-judge GMPP tracking has been introduced in [24] to reduce the searching voltage range. This method is based on the V_{OC} method with assumptions that the voltage and current of MPP are equal to 0.76 V of open circuit voltage and 0.9 A of short circuit current, respectively. Based on analysis of several partial shading patterns, it has been proved that this assumption is not always true. One well-known method based on the voltage zone skipping method is the maximum power trapezium (MPT) method [25].

Unfortunately, the modified MPT method reduced the range of voltage scanning only under narrow conditions. It did not solve the problems of the invisible zone under low temperatures and the minimum V_{OC} under high temperatures. In [26], an improved skipping mechanism was introduced, which divided the search range on the P-V curve into two equal zones to avoid scanning the other zone only if the operating voltage was initialized in the same zone containing the GMPP. However, the MPT method needs to scan the whole voltage range on the P-V curve. To ensure every peak was scanned, the researchers in [27] introduced a $0.8V_{ocmodel}$ jump method to make conventional MPPT algorithms work effectively under PSCs. The $0.8V_{ocmodel}$ jump method is an easy technique to implement and is considered a very effective global searching technique since only the closeness of the $0.8V_{ocmodel}$ zones is scanned rather than scanning the whole voltage range on the P-V curve. This technique is not always true, especially under a partially shaded and long string system. In such a case, the $0.8V_{ocmodel}$ method will scan the wrong zone and track the incorrect global peak [28].

Previous literature shows a need to reduce the scanning time for the GMPP to enhance the tracking performance. Despite the crucial progress that the modified MPPT methods have made, there is always a need to reduce the time consumed to reach the GMPP under PSC and to reduce the complexity of the MPPT algorithm. In this paper, the search skipping method is improved to neglect the searching voltage zones, ensuring that it has no GMPP. During GMPP tracking under PSCs, the automatic initial voltage generator algorithm ensures no overlap between two adjacent zones on the P-V curve. The proposed skipping algorithm guarantees that the GMPP is tracked accurately under all potential atmospheric circumstances with a shorter tracking time, and the ability to find the GMPP quickly will minimize the power loss due to full-scanning algorithms. In summary, the main contributions of this paper can be outlined in three forms:

- The algorithm is designed to provide an automatic and inclusive method to identify the accurate range locations of the GMPPs by analyzing the P-V curves under all potential atmospheric circumstances and generating a perfect initial voltage for the MPPT algorithm to ensure that there is no overlap between two adjacent zones on the P-V curve during GMPPT under PSCs.

- The proposed skipping algorithm is an improved version of the MPPT and $0.8V_{OC}$ methods, which work to neglect searching voltage zones that have no GMPP. This approach guarantees that the GMPP is tracked accurately under all potential atmospheric

TABLE I. PARAMETERS OF LR5-72HPH-525M PV MODULE [29]

Description	Value
Maximum power (P_{MPP})	525 W
Voltage at maximum power point (V_{MPP})	41.20 V
Current at maximum power point (I_{MPP})	12.75 A
Open circuit voltage (V_{OC})	49.05 V
Short circuit current (I_{sc})	13.65 A
Module efficiency (%)	20.5%
Temperature coefficient of I_{SC}	$+0.048\%/^{\circ}$C
Temperature coefficient of V_{OC}	$-0.270\%/^{\circ}$C
Temperature coefficient of P_{MPP}	$-0.350\%/^{\circ}$C

circumstances with a shorter tracking time.

- The proposed algorithm is also designed to have the ability to find the GMPP quickly and avoid scanning unnecessary zones. It solves the problems of overlap between two adjacent zones and scans the full range of the P-V curve.

II. METHODOLOGY

The PV module used in this project is LR5-72HPH-525M. The PV module parameters that are under standard test conditions of temperature = 25°C and solar irradiation = 1000 W/m^2 are given in Table I.

The proposed algorithm consists of two main parts: the accurate range of the GMPPs location algorithm and the skipping GMPPT algorithm, as shown in Fig. 1 and Fig. 2, respectively. The accurate range of the GMPPs location algorithm is an analysis process used to identify the accurate range locations of the GMPPs based on deep analysis of the P-V curves under all potential atmospheric circumstances. This part starts by injecting the number of series PV modules (N_s) and setting the maximum and minimum boundaries of the irradiance and ambient temperature. The simulation modules run with all potential different values of irradiances; in this case, 4000 different patterns were generated randomly to cover all potential PSC patterns without repeating any of them. For each generated pattern, the proposed algorithm measures the PV voltage (V_{PV}) and current (I_{PV}) and calculates the PV power (P_{PV}). From the V_{PV} and P_{PV} that have been calculated, the accurate range algorithm generates the PV-curves for each pattern (under temperature = 25°C) and calculates the GMPP and the corresponding voltage V_{MPP} for each automatically without any manual calculations and considers it as a reference voltage (V_{ref}).

After generating all patterns, the off-time analysis algorithm collects all module irradiances $[G_1, G_2, \ldots, G_{NS}]$ with calculated V_{MPP} in a data array. This array is arranged

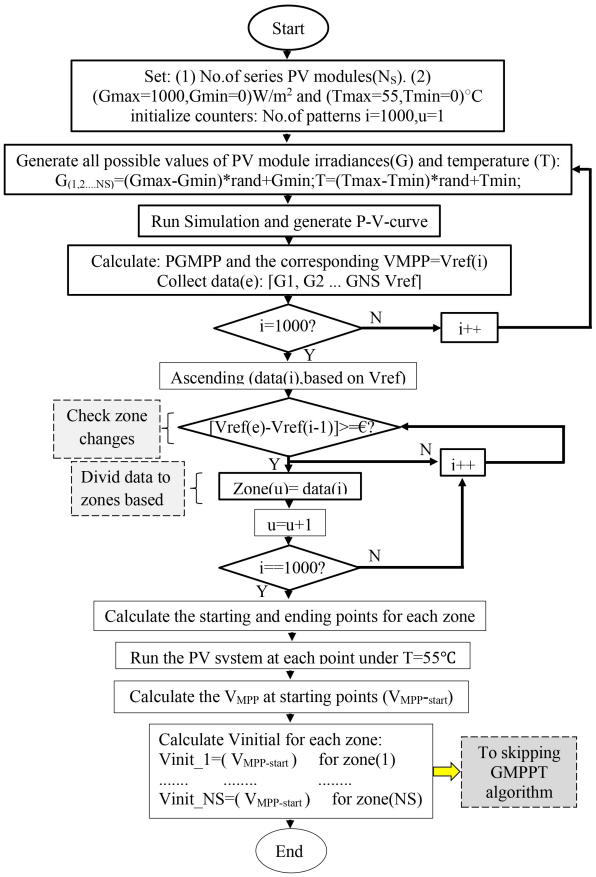

Fig. 1. The flowchart of the accurate range of the GMPPs location algorithm.

in ascending mode, depending on the V_{MPP} values, to divide it into N_S groups (V_{ref-1} to V_{ref-NS}) by searching for any significant difference between two adjacent values of V_{MPP} and apply the condition $(V_{ref(i)} - V_{ref(i-1)} \geq \varepsilon?)$. ε is a small value less than $0.1 \times V_{OCmodule}$. Because the accurate range algorithm takes many iterations, i.e., more than 1000 patterns, the GMPP jumped to another zone if the ΔV_{ref} increased more than ε. Thus, the initial voltages can be classified based on the GMPPs zones. The last step of this part generates the initial voltages and sends them to the skipping GMPPT algorithm. Suppose the algorithm generates the initial voltage under STC. In that case, a mismatch problem will occur when the ambient temperature converts from low to high level, and that would cause a wrong zone selection. To solve this problem, the algorithm generates the initial voltages under exceedingly high temperatures (Temp = 55°C) at the starting point of each zone. In this case, the algorithm avoided the wrong range zone. To avoid the mismatch under low temperatures, the proposed algorithm selects the middle points of the initial

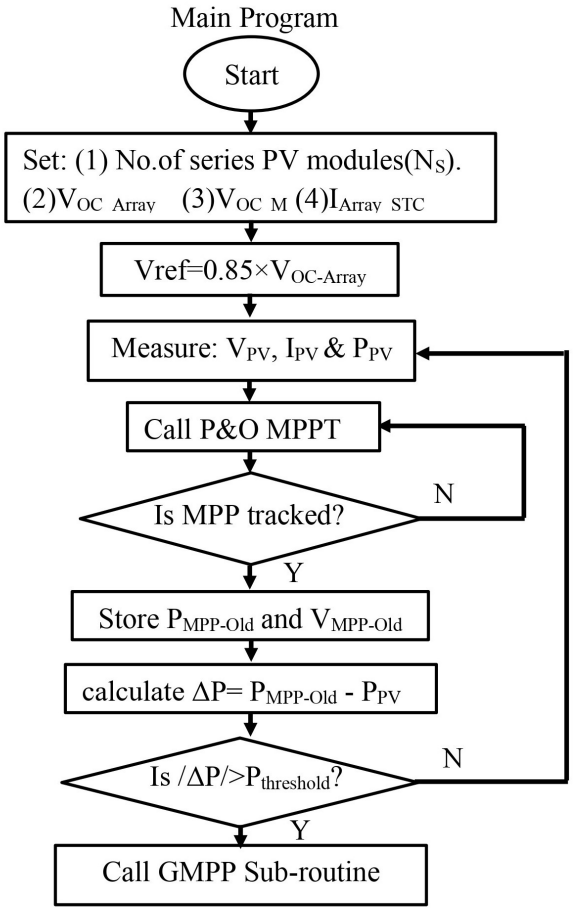

Fig. 2. The flowchart of skipping GMPPT algorithm.

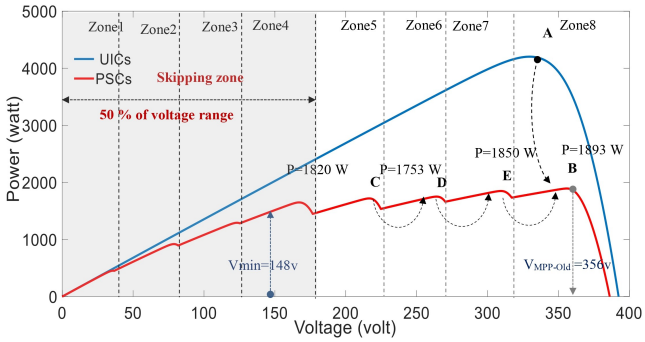

Fig. 3. The skipping GMPPT algorithm works under operation point changes from UIC to PSC scenario.

voltages for each zone to be remarkably close to the MPP.

To understand the skipping GMPPT algorithm, MATLAB simulation is conducted by assuming that a partial shading had just been reached, as shown in Fig. 3, which shifts the operating point from MPP (point A) under UIC to LMPP (point B) under PSC pattern. The proposed skipping GMPPT algorithm consists of a GMPP sub-routine, zone location sub-routine and Perturb and Observe (P&O) MPPT algorithm. The first step of this algorithm starts by taking some manufacturer parameters, N_S, $V_{OC-Array}$, V_{OC-M} and $I_{Array-STC}$. N_S is the number of PV modules connected in series, $V_{OC-Array}$ is the whole PV system's open circuit voltage, and $I_{Array-STC}$ is the maximum power point current under standard test conditions. All these parameters are provided by the manufacturer. The next step is to set a reference voltage to 0.85 $V_{OC-Array}$ to push the PV system to operate close to the MPP under UICs. Under UICs, the P&O MPPT algorithm works perfectly, and there is no need to use the GMPPT technique. Therefore, the algorithm calls the conventional P&O MPPT algorithm and stores the power and voltage of the MPP as ($P_{MPP-Old}$ and $V_{MPP-Old}$). Then, the program tracks the variation in power (ΔP), which indicates partial shading. The value of threshold power ($P_{threshold}$) must be selected wisely to avoid detecting small irradiance variations or detecting only large shadows. If the absolute value of ΔP reaches the $P_{threshold}$, the algorithm calls the GMPP subroutine for tracking the GMPP (Fig. 4). The $P_{threshold}$ is between 5 and 10% of the array's output power under STCs.

As shown in Fig. 4(a), the GMPP sub-routine algorithm starts by resetting the counters and minimum voltage (V_{min}), then calls the P&O algorithm. When an LMPP is tracked (point B), it will store the information of this point, the maximum power point of array power and voltage as $P_{MPP-Old}$ and $V_{MPP-Old}$, respectively. Hence, the zone location subroutine, as shown in Fig. 4(b), is called to determine the location of LMPP and point B on the P-V curve and ensure not to track it again in subsequent operations. To find the location of point B, the following test condition is applied on the $V_{MPP-Old}$ at this point:

$$m \times 0.95V_{OC-M} \leq V_{MPP-Old} \geq n \times 0.95V_{OC-M} \qquad (1)$$

where $n(n = 0,1,\ldots,N_{S-1})$ and $m(m = 1,2,\ldots,N_S)$ are variable counters representing each zone's start and end point on the P-V curve. The zone location subroutine is applied only once in each GMPP sub-routine call. By referring to Fig. 3, since point B is in zone 8, $V_{MPP-Old}$ = 356 V. The condition will continue to be tested, and the values of m and n will be increased until both reach $m = 7$ and $n = 8$. After the location of point B is calculated, the zone location subroutine stores the zone's number, $z = n$, in this case, $z = 8$, and then returns to the GMPP sub-routine. The next step is to determine the bounds of the voltage zone on the P-V curve where the GMPP cannot be found. The minimum voltage skipping range, V_{min}, represents the voltage value on the P-V curve, which can

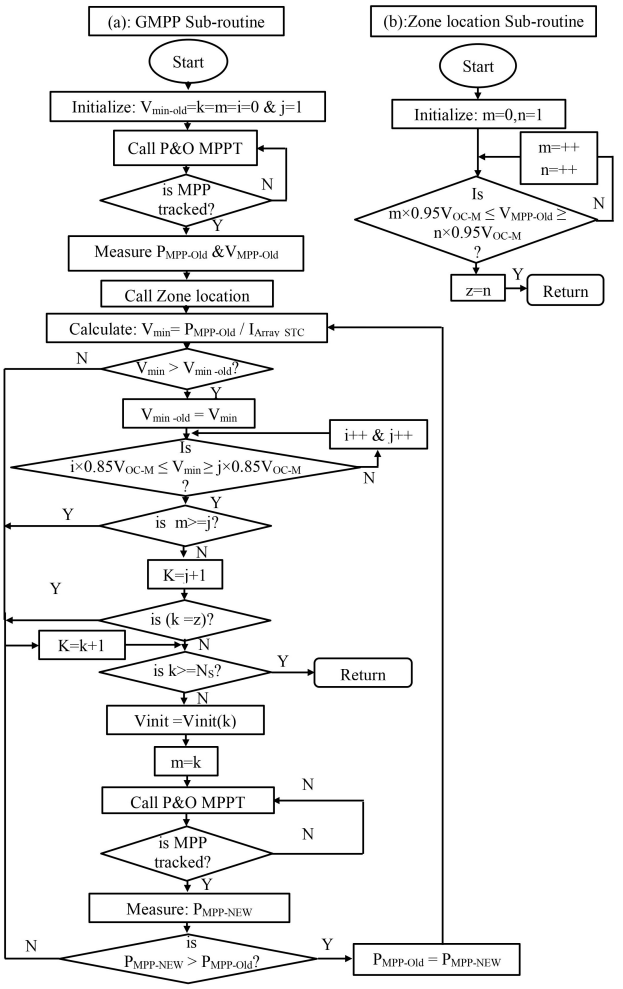

Fig. 4. The flowchart of (a) the GMPP sub-routine algorithm and (b) the zone location sub-routine.

guarantee there is no GMPP before it. $I_{MPP,STC,Array}$ bound the minimum voltage range to the $P_{MPP,STC,Array}$ according to (2).

$$V_{range,min} = \frac{P_{MPP,STC,Array}}{I_{MPP,STC,Array}} \tag{2}$$

As shown in Fig. 3, the value of V_{min} at the first scanning step is equal to 148 V, and this means there is no need to scan zones 1, 2, 3 and 4, which reduces the scanning time to approximately 50% of the voltage range on the P-V curve. After the V_{min} has been determined, the value of V_{min} is compared with $V_{min-old}$, which comes from a previous step, where the higher value is chosen (the higher the value of V_{min}, the fewer peaks to search). In this step, the condition $V_{min} > V_{min-old}$ holds, and the GMPP sub-routine leads to updating the value of $V_{min-old}$. Then, the program determines the neglected scanning zones by applying the condition in (3).

$$i \times 0.85V_{OC-M} \leq V_{min} \geq j \times 0.85V_{OC-M} \tag{3}$$

Since the V_{min} is in zone 4, the condition will continue to be tested with an increase of the counters (i, j) until it reaches $i = 3$ and $j = 4$, where the voltage value is $V_{min} = 148$V. To avoid re-scanning of zone 8, which contains point B, the GMPP sub-routine tests the condition if k is equal to z, where z is the number of zones which contain point B. If the condition is met, the algorithm finds this zone and moves to the next by increasing i and j. From analysis and observation, it was found that the zone containing V_{min} does not contain GMPP within it, except in the case of V_{min}, which comes from $P_{GMPP}/I_{Array,STC}$. There is no need to scan this zone because it was already scanned. Therefore, the algorithm will test another condition, if $k = j$, to avoid tracking the V_{min} zone. If one of these conditions is not met, the algorithm will select the zone initial voltage V_{min} of zone 5 in this scenario to start tracking for the GMPP within this zone.

The algorithm scans zone 5 for a potential GMPP by calling the P&O algorithm. After ensuring that the P&O algorithm tracked the MPP in zone 5, equal to 1820 W, the sub-routine stored this value as $P_{MPP-NEW}$. The new power is compared with the old one from the last sample, $P_{MPP-Old}$. If the $P_{MPP-Old}$ is larger than the $P_{MPP-NEW}$, the GMPP sub-routine jumps to the next zone by increasing the values of i and j, where the $P_{MPP-Old}$ value remains unchanged. On the other hand, if the $P_{MPP-Old}$ is lower than $P_{MPP-NEW}$, the $P_{MPP-Old}$ is updated, and the GMPP sub-routine jumps to the next zone. After jumping to any new zone, the algorithm calculates and compares the V_{min} value with the previous sample. If the new V_{min} exceeds the previous one, the GMPP sub-routine updates the skipping voltage range. These steps repeat until the number of zones reaches the number of series PV modules (N_S), then return to the main program and repeat the same procedures. This proposed algorithm would reduce the tracking time, where it does not need to scan the whole P-V curve and immediately neglect four zones, which are guaranteed not to contain the GMPP. Neglecting four zones means minimizing more than 50% of the scanning time and just needing to scan less than 50% of the P-V curve. Also, it is obvious from the deep analysis and observations that there is no GMPP with the V_{min} within, which also reduces the tracking time by an extra one zone.

III. Simulation Results

To verify the proposed skipping MPPT algorithm efficiency, simulation results were conducted using MATLAB/SIMULINK supported by an M-file code. Two

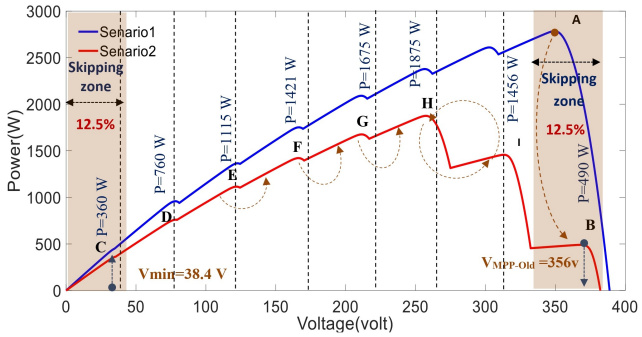

Fig. 5. The P-V curve under partial sudden change from scenario 1 to scenario 2

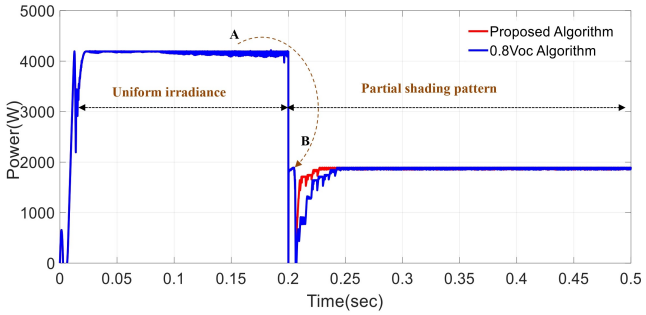

Fig. 7. Comparison of PV output power under the scenario shown in Fig. 3

MPPT methods, the $0.8V_{OC-M}$ method and the proposed skipping algorithm, have been tested under different PSCs where eight irradiation levels are applied on the PV string. To analyze the ability of the proposed skipping algorithm in neglecting zones under the lowest value of V_{min} when V_{min} is located at zone 1 ($V_{min} = 490/12.75 = 38.4$ V), the scenario of Fig. 5 has been tested. It is observed that each P-V curve has 8 peaks, and the MPPT algorithm needs to scan all these peaks to decide which one represents the GMPP.

To highlight the advantages of the proposed skipping MPPT algorithm under varying ambient temperatures (from 10°C to 25°C), the partial shading scenario shown in Fig. 6 has been tested. When the ambient temperature changes, the P-V curve shifts towards the left in case of a decrease or the right in case of an increase, and this will affect the voltage operation point on the P-V curve. However, the $0.8V_{OC-M}$ method is ineffective under all temperature ranges since the V_{OC-M} is a fixed value. Fig. 7 shows the PV output power for

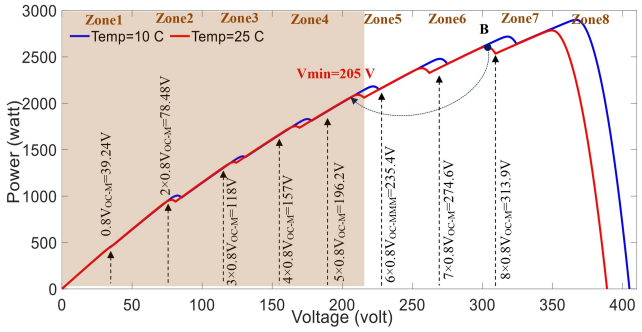

Fig. 6. The P-V curve scenario under different temperatures (10°C and 25°C)

the proposed skipping algorithm compared with the $0.8V_{OC-M}$ algorithm, where the scenario shown in Fig. 3 has been used. It is obvious from Fig. 7 that both algorithms tracked the MPP under UIC, which represents point A (P_{MPP} = 4200 W), as well as the GMPP, point B (P_{GMPP} = 1893 W), under PSC and avoided other LMPPs. The proposed skipping MPPT algorithm reached GMPP point B at a very high speed with minimum fluctuations around the GMPPs compared with the $0.8V_{OC-M}$ method.

To find out how the tracking process of GMPP occurred, a zoomed part of Fig. 7 is taken, as shown in Fig. 8. By referring to Fig. 3, the P-V curve under PSC contains eight peaks distributed over eight zones, and there is just one peak representing the GMPP. To determine which peak represents the GMPP, the algorithm should scan all eight peaks and select the one with the largest power. When the partial shading occurred at t = 0.2 sec, the operational point jumped from point A to point B, where the proposed skipping algorithm tracked the MPP around this point and calculated the $V_{min} = 1890/12.75 = 148.2$V, as shown in Fig. 3. The proposed algorithm ignored scanning the zone which contains the V_{min} (zone 4 in this scenario) and all zones before it (zones 1, 2 and 3). As shown in Fig. 8, the proposed algorithm must track only zones 5, 6 and 7. Zone 8 was already scanned at point B, which means the scanning process only acquires 50% of the voltage range on the P-V curve. Both techniques have tracked the GMPPs under PSC, but the proposed skipping MPPT algorithm is superior in tracking speed, where the time difference between the two techniques is 16.6 msec. The output power for both techniques under PSC is 1890 W compared with the global maximum power point of 1993 W. The MPPT efficiency is remarkably high, reaching 99.84%. For a clear comparison, the perturbation step size was chosen optimally as 0.5 V for both techniques. The simulation results shown in Fig. 8 substantiate that the effectiveness of the proposed skipping MPPT algorithm has been superior compared with the $0.8V_{OC-M}$ algorithm in terms of tracking speed to reach the GMPP under PSCs.

Fig. 9 shows the PV output power for the proposed skipping algorithm compared with the $0.8V_{OC-M}$ algorithm, where the scenarios shown in Fig. 5 have been applied.

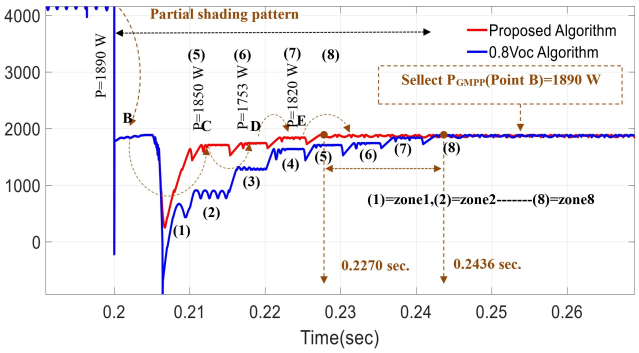

Fig. 8. Zoomed view of Fig. 7 due to changes from UIC to PSC scenario at t = 0.2 sec

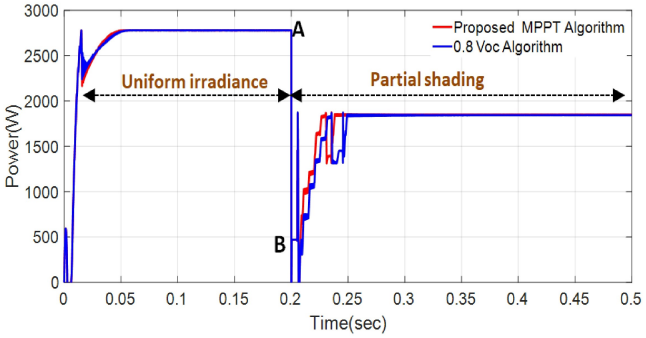

Fig. 9. Comparison of PV output power under the scenario shown in Fig. 5

Both algorithms tracked the GMPP under two PSC scenarios, which represent point A (scenario 1) and the GMPP, point B (scenario 2), and avoided all LMPPs. The proposed algorithm reached GMPP point B with a good tracking speed performance and can quickly track the GMPP compared to the $0.8V_{OC-M}$ algorithm, with a time difference of 16 msec.

Fig. 10 shows the zoomed view of Fig. 9 for the time interval of 0.19 to 0.26 sec. It shows how both algorithms track the GMPP when the sudden partial shading occurs at t = 0.2 sec. Due to the sudden partial shading, the operating point on the P-V curve shifts to point B, which represents an LMPP and is considered the reference GMPP. As shown in Fig. 10, the proposed algorithm immediately calculates the V_{min} value, specifying the tracking start point, and neglects all zones located before it. In this case, the proposed algorithm starts scanning point D while point C has been ignored. As peak D exceeds peak B, the algorithm updates its reference GMPP information, and point D is now considered the reference GMPP for the next zone.

Similarly, with four more zones (peak E to peak H), the algorithm updates its reference GMPP information, and peak H is now considered the reference GMPP for the next zone. Then, when peak I is reached, which is smaller than peak H, the proposed algorithm does not update its reference GMPP information and peak H is still considered the reference GMPP. For the proposed algorithm, there is no need to scan point B because it is already being scanned when the sudden partial shading occurs. The $0.8V_{OC-M}$ algorithm scanned all 8 zones, from an initial point to the ending operation point, while the proposed algorithm ignored scanning zone B and zone C, which means minimizing the tracking time by 25%.

Fig. 11 shows the PV output power for the proposed algorithm compared with the $0.8V_{OC-M}$ algorithm under two different temperatures: a) 25°C and b) 10°C based on the scenario shown in Fig. 6. As shown in Fig. 11(a), both algorithms tracked the GMPP under 25°C, which is in the eighth zone, but the proposed algorithm is superior in term of fast-tracking with Δt = 27 msec. When the ambient temperature has been changed to 10°C (see Fig. 11(b)) under the same partial shading pattern, the $0.8V_{OC-M}$ algorithm fails to track the GMPP because it has been too busy to track the LMPP (point B), instead of the GMPP. This is an example of how the $0.8V_{OC-M}$ algorithm fails to track the GMPP under different ambient temperatures, even if the partial shading pattern remains the same. The overall simulation results substantiate the effectiveness of the proposed skipping MPPT algorithm compared to the $0.8V_{OC-M}$ algorithm in terms of tracking speed and the accuracy of identifying the GMPP under PSCs.

IV. Experimental Results

To validate the effectiveness of the proposed MPPT algorithm in tracking the GMPP, the proposed optimum voltage range MPPT algorithm has been implemented using an experimental setup as shown in Fig. 12. The single printed circuit board (PCB) which consists of a boost converter, SiC MOSFET gate driver circuit, isolated (20V/-5V) power supply, STM32F334R8 microcontroller and voltage and current

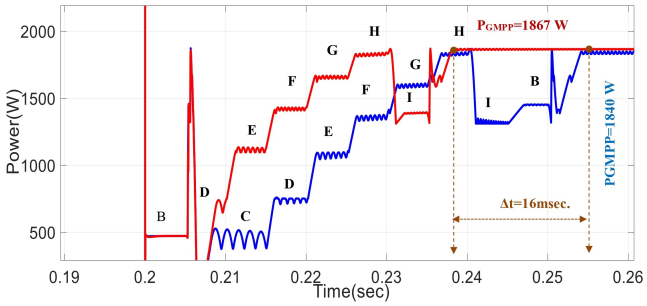

Fig. 10. Zoomed view of Fig. 9 due to changes from scenario 1 to scenario 2 at t = 0.2 sec

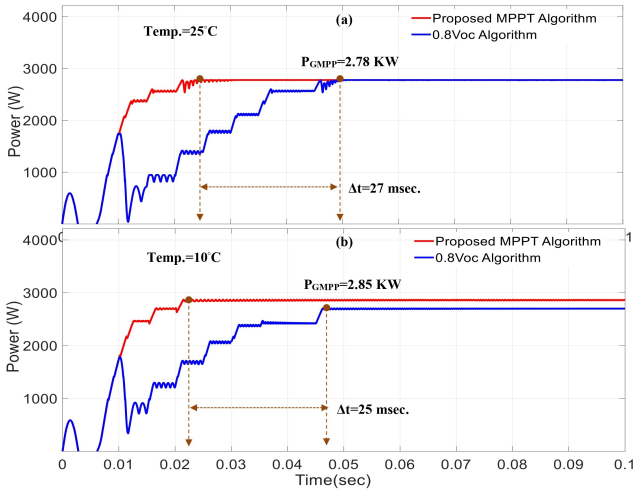

Fig. 11. Comparison of PV output power under partial shading scenario shown in Fig. 10 at a) Temp = 25°C and b) Temp = 10°C.

TABLE II. PARAMETERS OF LR5-72HPH-525M

Description	Value
Inductor (L)	1.2 mH
Input capacitor (C_{in})	4.7uF/1200V × 2
DC bus capacitor (C_{out})	1000uF/450V × 2
Switching Frequency (f_{sw})	50 kHz

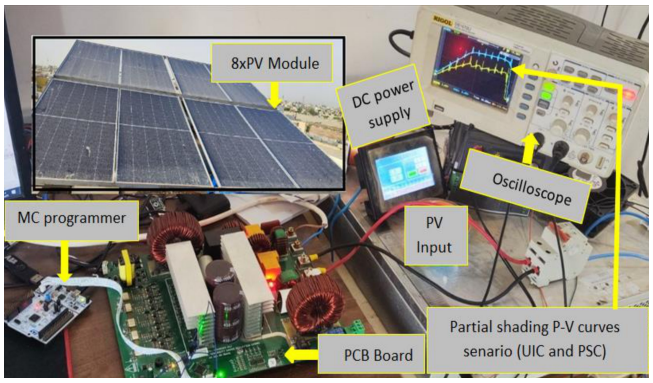

Fig. 12. The experimental hardware setup.

sensors, have been designed using Proteus 8 Professional program. The eight (LR5-72HPH-525M) solar panels were connected to a dc load via a boost converter. The practical boost converter parameters shown in Table II have been designed carefully using a standard equation to be compatible with the solar array rated power. To draw the practical power response in the oscilloscope, the output voltage of the DAC is changed from 0 to 3.3 V, and a 6.5 × non-inverting op-amp has been inserted between the DAC and the oscilloscope to function as a buffer and protect the MCU from any possible short-circuit current. So, the full scale is 3.3 V × 6.5 = 21.45 V, which equals a rated power of 4.2 kW. The oscilloscope reading represents 0.196 kW/V.

Fig. 13 shows the PV output power of the proposed skipping algorithm compared to the $0.8V_{OC-M}$ algorithm under different weather conditions where the partial shading occurred at t = 16 and t = 6 sec for Fig. 13 (a and b), respectively. Both algorithms tracked the MPP, P_{MPP} = 2.665 kW and P_{MPP} = 3.78 kW, for Fig. 13 (a and b). Under UIC, both algorithms tracked the uniform MPP at the same tracking speed, while under partial shading scenarios, the proposed skipping MPPT algorithm is superior in terms of tracking speed to reach the GMPP. The tracking time difference between them is approximately 3.28 and 0.78 sec for Fig. 13 (a and b), respectively.

After partial shading occurs, the proposed algorithm's operating point has been shifted from point A to point B. In the partial shading scenario, the proposed algorithm measured the MPP at point B and then calculated the V_{min} value according to (2). As shown in Fig. 13(a) and according to the $0.8V_{OC-M}$ theory, the 131 V is located at zone 3 on the P-V curve, which means that zone 3 and all zones located before it have been ignored. Neglecting the scan of the first three zones means that the proposed algorithm neglects approximately 38% of the voltage range, decreasing the scanning time to less than 62%. Also, based on the value of V_{min} shown in Fig. 13(b), the number of neglecting zones is five, which leads to neglecting approximately 62% of the tracking time. The overall experimental results shown in Fig. 13 (a and b) substantiate the effectiveness of the proposed skipping MPPT algorithm compared to the $0.8V_{OC-M}$ algorithm in terms of GMPP tracking speed by neglecting unnecessary scanning zones.

Fig. 14 shows the PV output power of the proposed skipping algorithm compared to the $0.8V_{OC-M}$ algorithm under different shading scenarios where the partial shading occurred at t = 15 sec. From the values of V_{min}, it is obvious that the proposed algorithm ignored scanning the first four zones, which leads to a decrease in the scanning time to approximately 50%. The main reason behind the considerable number of neglected zones, 4 zones, in this case, is that operating point B has been located at the GMPP. Under UIC, both algorithms tracked the MPP simultaneously, while under partial shading scenarios, the $0.8V_{OC-M}$ algorithm fails to track the GMPP because it has been busy tracking the LMPP instead of the GMPP. Fig. 14 shows how the $0.8V_{OC-M}$ algorithm fails to track the GMPP under PSCs. The main reason behind the inability of the $0.8V_{OC-M}$ algorithm to track the GMPP is its incompetence in accurately determining the perfect voltage ranges for each zone, which causes

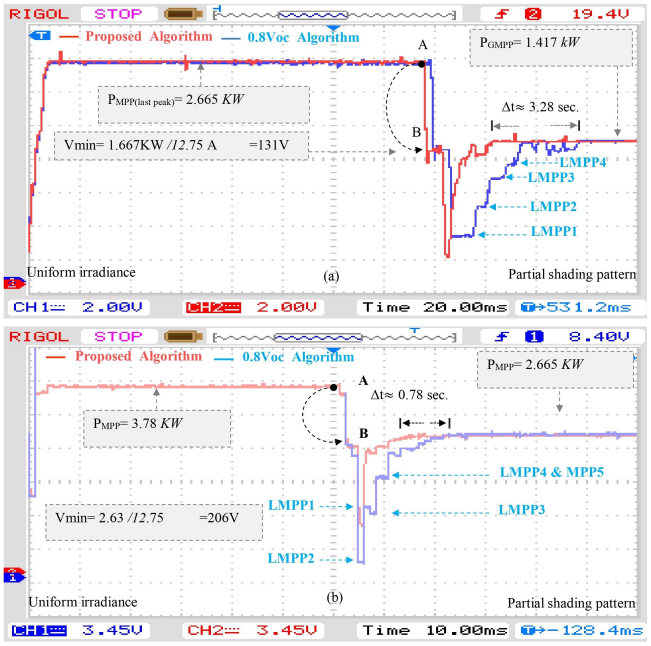

Fig. 13. Experimental PV output power of proposed skipping algorithm compared with $0.8V_{OC-M}$ algorithm under UIC and PSC based on tracking speed; a) Scenario 1, b) Scenario 2.

interference in adjacent zones. As shown in Fig. 14, the interference in adjacent zones leads to tracking the wrong LMPP (zone 7) instead of the GMPP (zone 8), which causes a power loss of P = 196 W.

V. Conclusion

This paper has a comparative analysis of the P-V curves under all potential atmospheric circumstances. It proves graphically and mathematically that the idea that peaks should be located around the multiples of $0.8V_{OC-M}$ is not always true. Under temperature variation and extreme partial shading patterns, the peaks move from one to another, which causes a large deviation of the multiples of the $0.8V_{OC-M}$ locations. Also, the $0.8V_{OC-M}$ needs to scan the whole voltage range of the P-V curve to find the GMPP, which is considered time-consuming. To overcome these weak points, an algorithm to identify the accurate range locations of the GMPPs and an improved skipping zones MPPT algorithm are proposed. The simulation and experimental results show that the proposed skipping MPPT algorithm has superiorly tracked the GMPPs under PSCs at all locations compared with the $0.8V_{OC-M}$ algorithm. The proposed MPPT algorithm harvested higher PV power with faster tracking speed. Under 10°C, the $0.8V_{OC-M}$ algorithm fails to track the GMPP because it selected the wrong peak (point B) instead of the GMPP with power losses of 196 watts. While under 25°C, the

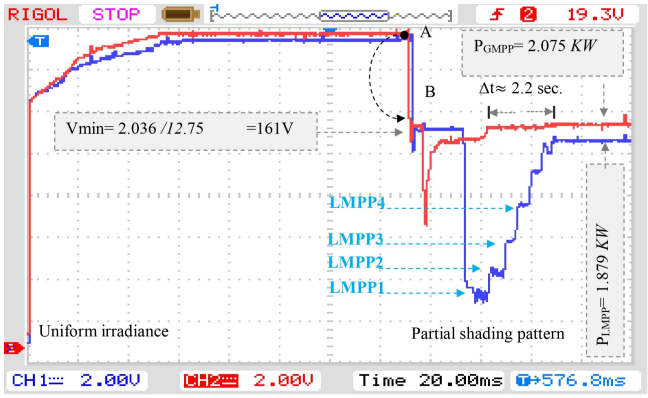

Fig. 14. Experimental PV output power of proposed skipping algorithm compared with $0.8V_{OC-M}$ algorithm under UIC and PSC Scenario 3.

proposed method takes less time than the $0.8V_{OC-M}$ algorithm to reach the GMPP, where the time difference between them is $\Delta t = 27$ msec.

Acknowledgment

The authors thank the Universiti Sains Malaysia and the University of Technology, Baghdad, Iraq, for the research collaboration that completed this project.

Conflict of Interest

The authors declare no conflict of interest.

References

[1] A. Chikh and A. Chandra, "An optimal maximum power point tracking algorithm for PV systems with climatic parameters estimation," *IEEE Trans. on Sustainable Energy*, vol. 6, no. 2, pp. 644–652, 2015.

[2] K. S. Tey and S. Mekhilef, "Modified incremental conductance algorithm for photovoltaic system under partial shading conditions and load variation," *IEEE Trans. on Industrial Electronics*, vol. 61, no. 10, pp. 5384–5392, 2014.

[3] A. Ostadrahimi and Y. Mahmoud, "Novel spline-MPPT technique for photovoltaic systems under uniform irradiance and partial shading conditions," *IEEE Trans. on Sustainable Energy*, vol. 12, no. 1, pp. 524–532, 2021.

[4] J. Dadkhah and M. Niroomand, "Optimization methods of MPPT parameters for PV systems: Review, classification, and comparison," *J. of Modern Power*

Systems and Clean Energy, vol. 9, no. 2, pp. 225–236, 2021.

[5] M. Y. Heelan and F. A. M. Al-Qrimli, "Design and simulation of neuro-fuzzy based MPPT controller for PV power system," in *2nd Int. Conf. on Electrical, Communication and Computer Engineering (ICECCE), Turkey*, pp. 1–6, June 2020.

[6] X. Zhang, D. Gamage, B. Wang, and A. Ukil, "Hybrid maximum power point tracking method based on iterative learning control and perturb & observe method," *IEEE Trans. on Sustainable Energy*, vol. 12, no. 1, pp. 659–670, 2021.

[7] R. B. Bollipo, S. Mikkili, and P. K. Bonthagorla, "Hybrid, optimal, intelligent and classical PV MPPT techniques: A review," *CSEE J. of Power and Energy Systems*, vol. 7, no. 1, pp. 9–33, 2021.

[8] K. Amara, A. Fekik, E. Bourennane, T. Bakir, and A. Malek, "Improved performance of a PV solar panel with adaptive neuro fuzzy inference system ANFIS based MPPT," in *7th Int. Conf. on Renewable Energy Research and Applications ICRERA, France*, pp. 1098–1101, Oct 2018.

[9] H. M. Abd-Alhussain and N. Yasin, "Modeling and simulation of solar PV module for comparison of two MPPT algorithms (P&O & INC) in MATLAB/simulink," *Indonesian J. of Electrical Engineering and Computer Science*, vol. 18, no. 2, pp. 666–667, 2020.

[10] M. Farsi and J. Liu, "Nonlinear optimal feedback control and stability analysis of solar photovoltaic systems," *IEEE Trans. on Control Systems Technology*, vol. 28, no. 6, pp. 2104–2119, 2020.

[11] S. Lyden, H. Galligan, and M. E. Haque, "A hybrid simulated annealing and perturb and observe maximum power point tracking method," *IEEE Systems Journal*, vol. 15, no. 3, pp. 4325–4333, 2021.

[12] M. Haziq, M. Norfauzi, and S. M. Sulthan, "Optimizing step-size of perturb & observe and incremental conductance MPPT techniques using PSO for grid-tied PV system," *IEEE Access*, vol. 11, pp. 13079–13090, 2023.

[13] N. Kumar, I. Hussain, B. Singh, and B. K. Panigrahi, "Framework of maximum power extraction from solar PV panel using self-predictive perturb and observe algorithm," *IEEE Trans. on Sustainable Energy*, vol. 9, no. 2, pp. 1–9, 2018.

[14] S. Bhattacharyya, P. Dattu, K. Sampath, S. Samanta, and S. Mishra, "Steady output and fast tracking MPPT (SOFT-MPPT) for P&O and InC algorithms," *IEEE Trans. on Sustainable Energy*, vol. 12, no. 1, pp. 293–302, 2021.

[15] I. Pervez, I. Shams, and S. Mekhilef, "Most valuable player algorithm based maximum power point tracking for a partially shaded PV generation system," *IEEE Trans. on Sustainable Energy*, vol. 12, no. 4, pp. 1876–1890, 2021.

[16] M. Dhimish, P. Mather, and V. Holmes, "Novel photovoltaic hot-spotting fault detection algorithm," *IEEE Trans. on Device and Materials Reliability*, vol. 19, no. 2, pp. 378–386, 2019.

[17] W. P. Lamb, D. E. Asnes, J. Kupfer, and E. Lickey, "Real-time anticipation and prevention of hot spots by monitoring the dynamic conductance of photovoltaic panels," *IEEE J. of Photovoltaics*, vol. 12, no. 4, pp. 1051–1057, 2022.

[18] S. Xu, Y. Gao, G. Zhou, and G. Mao, "A global maximum power point tracking algorithm for photovoltaic systems under partially shaded conditions using modified maximum power trapezium method," *IEEE Trans. on Industrial Electronics*, vol. 68, no. 1, pp. 370–380, 2021.

[19] R. M. Ahmed, N. E. Zakzouk, M. I. Abdelkader, and A. K. Abdelsalam, "Modified partial-shading-tolerant multi-input-single-output photovoltaic string converter," *IEEE Access*, vol. 9, pp. 30663–30676, 2021.

[20] K. Chen, S. Tian, Y. Cheng, and L. Bai, "An improved MPPT controller for photovoltaic system under partial shading condition," *IEEE Trans. on Sustainable Energy*, vol. 5, no. 3, pp. 978–985, 2014.

[21] G. C. Hsieh, H. I. Hsieh, C. Y. Tsai, and C. H. Wang, "Photovoltaic power-increment-aided incremental - conductance MPPT with two-phased tracking," *IEEE Trans. on Power Electronics*, vol. 28, no. 6, pp. 2895–2911, 2013.

[22] M. E. Basoglu, "Module level global maximum power point tracking strategy," in *4th Int. Conf. on Power Electronics and their Applications (ICPEA), Turkey*, pp. 1–5, Sept 2019.

[23] K. Sundareswaran, P. Sankar, P. S. R. Nayak, S. P. Simon, and S. Palani, "Enhanced energy output from a PV system under partial shaded conditions through artificial

bee colony," *IEEE Trans. on Sustainable Energy*, vol. 6, no. 1, pp. 1–12, 2015.

[24] Y. Wang, Y. Li, and X. Ruan, "High accuracy and fast speed MPPT methods for PV string under partially shaded conditions," *IEEE Trans. on Industrial Electronics*, vol. 63, no. 1, pp. 235–245, 2015.

[25] A. M. S. Furtado, F. Bradaschia, M. C. Cavalcanti, and L. R. Limongi, "A reduced voltage range global maximum power point tracking algorithm for photovoltaic systems under partial shading conditions," *IEEE Trans. on Industrial Electronics*, vol. 65, no. 4, pp. 3252–3262, 2018.

[26] M. Kermadi, Z. Salam, J. Ahmed, and E. M. Berkouk, "A high-performance global maximum power point tracker of PV system for rapidly changing partial shading condition," *IEEE Trans. on Industrial Electronics*, vol. 68, no. 3, pp. 2236–2245, 2020.

[27] H. Patel and V. Agarwal, "Maximum power point tracking scheme for PV systems operating under partially shaded conditions," *IEEE Trans. on Industrial Electronics*, vol. 55, no. 4, pp. 1689–1698, 2008.

[28] J. Ahmed and Z. Salam, "An improved method to predict the position of maximum power point during partial shading for PV arrays," *IEEE Trans. on Industrial Electronics*, vol. 11, no. 6, pp. 1378–1387, 2015.

[29] "LONGi Solar, LR5-72HPH 525-545M, Solar Panel Data Sheet." https://mesolarstores.com/wp-content/uploads/LONGI-525-545-Wp-datasheet.pdf.